Finite Element Modeling of HSS-to-HSS Moment Connections

M.F. Fadden & J.P. McCormick
University of Michigan, USA.

SUMMARY:
HSS members provide a possible alternative to typical wide flange seismic moment frame systems in low- to mid-rise structures. With an understanding of the limiting width-thickness and depth-thickness ratios for HSS beam members from previous studies, fully welded reinforced and unreinforced HSS-to-HSS seismic moment connections are studied using Abaqus finite element analysis software. The beam width-to-column width ratio is found to have an important effect on unreinforced connections, while diaphragm thickness and length affects the moment and equivalent viscous damping of reinforced connections. The findings indicate that connections with diaphragms better preserve desirable strong column-weak beam connection behavior under cyclic loads.

Keywords: steel systems, hollow structural sections (HSS), moment connections, seismic design

1. INTRODUCTION

Steel moment resisting frames (MRF) have been used throughout seismic regions because of their inherent ability to resist lateral forces through rigid frame action. Due to their ability to dissipate seismic energy in a ductile manner, steel MRFs are popular in seismically active regions. These frames are able to withstand large plastic deformations without significant degradation or development of instabilities that could lead to collapse (Roeder 2000). In the past, most research has focused on the utilization of moment frame systems composed of wide-flange members. However, hollow structural sections (HSS) have many desirable properties which make them suitable for use in MRFs in seismic regions including favorable bending, compression, and torsional resistance.

Currently, HSS are used in a number of building applications such as column members, bracing elements, truss members, exposed structural steel, and cladding supports. These applications exploit the favorable bending, compression, and torsional resistance of HSS. However, the use of HSS in seismic moment resisting frames typically has been limited to HSS columns or concrete filled tube (CFT) columns connected to wide flange beams (Hajjar 2000, Kurobane 2002, Packer 2000, Nishiyama and Morino 2004). HSS-to-HSS seismic moment resisting frames have the potential to reduce the seismic weight of a structure, limit lateral bracing requirements, and open new applications for HSS. To utilize HSS-to-HSS MRFs in seismic regions, an understanding of both the HSS beam behavior and connection details suitable for large inelastic cyclic loads must be developed.

1.1. Background

Several studies have considered the bending behavior of HSS beam members under monotonic loads. The results suggest that the width-thickness (b/t) and depth-thickness (h/t) ratios control the local buckling behavior and the moment capacity of HSS beam members (Korol and Hudoba 1972, Hasan and Hancock 1988, Wilkinson and Hancock 1998). To further the use of HSS in seismic regions, recent large-scale experimental testing of HSS beam members has considered the behavior of eleven different HSS members under cyclic bending loads (Brescia et al. 2009, Fadden and McCormick

2012a). Continuum finite element models have been developed and calibrated based on experimental testing utilizing measured material properties and capturing the local buckling behavior (Fadden and McCormick 2012b). The cyclic bending study results reiterate the importance of *b/t* and *h/t* observed during monotonic testing and provides a better understanding of the expected cyclic local buckling behavior.

HSS have been used extensively in planar and multi-planar truss connections and HSS column-to-wide flange beam connections. Research on HSS trusses has shown that the ratio of the width of the brace-to-the width of the chord governs the connection load carrying capacity (Davies et al. 1984, Koskimaki and Niemi 1990). As this ratio approaches 1.0, the failure mode changes abruptly because the webs of the chord stiffen the connection. While the use of HSS columns in the United States is limited, over 90% of steel buildings in Japan use HSS columns because of their ability to resist biaxial loads (Kurobane 2002). Since connections must behave in a rigid manner, unstiffened HSS columns are not acceptable (Packer and Henderson 1997). In Japan, a number of studies addressed this inadequacy by including internal and external connection diaphragms (Kamba and Tabuchi 1994) or by increasing the wall thickness (Kamba et al. 1994, Tanaka et al. 1996). Currently, design guides are available with recommendations for the design of HSS-to-HSS moment connections under static loads (Packer et al. 2009, AISC 2011) and seismic HSS-to-wide flange moment connections (Kurobane et al. 2004, AISC 2006).

HSS-to-HSS moment connection studies are limited. Many early studies of the behavior of HSS-to-HSS moment connections were performed on Vierenedeel truss connections. Unequal width connections are incapable of full moment transfer without reinforcement and are generally too flexible to be considered rigid moment connections (Korol et al. 1977). Experimental testing has shown that doubler plates, stiffeners, and haunches can improve performance in monotocally loaded connections. One study has considered the use of hollow sections built from channel sections for a seismic moment connection (Kumar and Rao 2006, Rao and Kumar 2006). This connection utilizes web openings to allow bolting and develops moment through shear lag in channel members welded to the column.

A significant amount of work has been undertaken in the finite element modelling of wide flange beam seismic moment connections. After the 1994 Northridge earthquake in the U.S., most studies focused on modelling the behavior of beam-to-column sub-assemblages (El-Tawil et al. 1998). These finite element models more closely examined the state of stress in connections that experienced large inelastic displacements and made recommendations for improved design details. Only a few models have been developed to consider HSS-to-HSS moment connection behavior. Korol and Mizra (1982) performed a study of 73 combinations of Vierendeel truss branch-to-chord connections considering their ability to transfer moment. The findings show that increasing the width of the brace from 40% to 80% of the chord width increases the moment capacity by 60%. More recent studies have considered the behavior of HSS connections, validating yield line theory approaches (Kosteski et al. 2002).

1.2. Objective

The finite element analysis study described in this paper addresses the ability of HSS-to-HSS moment connections to form stable plastic hinges under large cyclic inelastic deformations. A parametric study of 133 HSS beams allows for the determination of limiting depth-thickness (*h/t*) and width-thickness (*b/t*) ratios based on a finite element model calibrated to experimental results. Utilizing these limiting ratios, reinforced and unreinforced HSS-to-HSS moment connections are developed. The effect of the beam width-to-column width ratio (β) and beam depth are considered for the unreinforced connection. The use of internal and external diaphragms is then examined to better understand their ability to develop the full moment capacity of the HSS beam member and achieve desirable strong column-weak beam behavior. The diaphragm thickness (t_d) and length (l_d) are examined for their ability to improve the performance of the connection under cyclic loads. This study provides insight into connection configurations that are likely suitable for HSS-to-HSS moment connections for seismic applications.

2. HSS BEAM BENDING BEHAVIOR

2.1 Parametric study beam model setup

A parametric study is undertaken to consider the effect of the *b/t* and *h/t* ratios on the local buckling and cyclic hysteretic HSS bending behavior. The parametric study considers HSS beams with sizes between HSS 152.4x50.8x4.8 and HSS 508.0x304.8x15.9, providing a large set of sections and a wide range of widths, depths, and thicknesses. The wide range of sections allows for consideration of the effect of local buckling on the degradation of the maximum moment capacity with respect to *b/t* and *h/t*. The results allow for a better understanding of the parameters that limit stable plastic hinge formation. The HSS members used in the parametric cyclic bending study are modelled using Abaqus FEA (DSS 2008). The beam finite element model (FEM) is calibrated to eleven experimentally tested sections (Fadden and McCormick 2012b) utilizing experimentally tested material properties and geometric imperfections (Fig. 2.1).

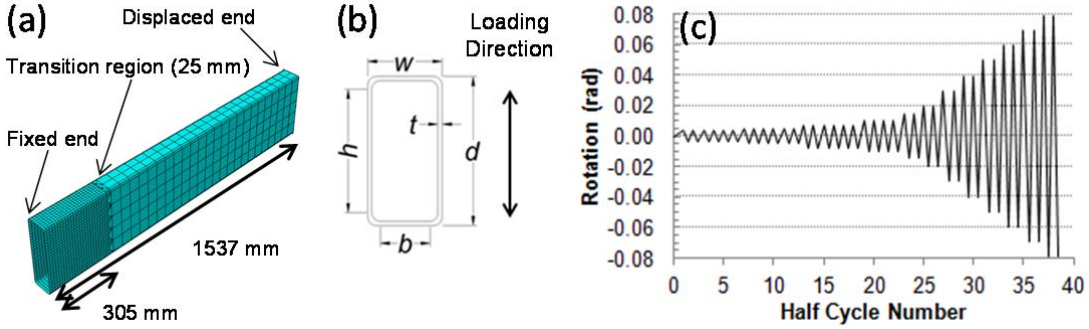

Figure 2.1 HSS finite element beam parametric study: (a) beam FEM, (b) cross-section dimensions, and (c) cyclic loading protocol.

2.2 HSS cyclic bending behavior

The cyclic hysteretic behavior is dependent on the *b/t* and *h/t* ratios. An increase in the *b/t* or *h/t* ratio causes an increase in the amount and rate of degradation of the moment capacity of the HSS beam. Fig. 2.1 plots the percent degradation of the maximum moment capacity from the overall maximum moment to the moment capacity obtained during the 0.04 rad. cycle with respect to the *b/t* (Fig. 2.2a) and *h/t* (Fig. 2.2b) ratios.

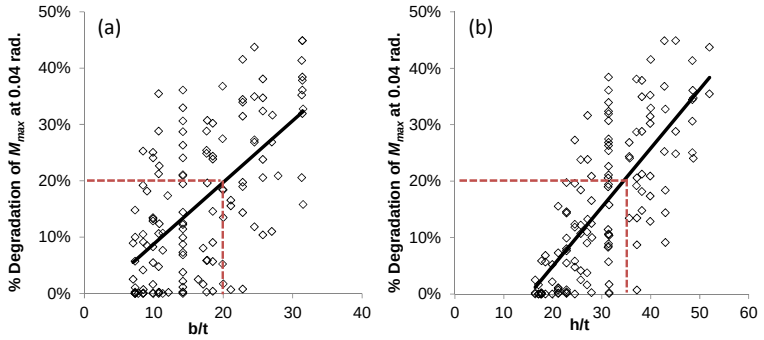

Figure 2.2 Percent degradation of M_{max} at 0.04 rad. with respect to (a) *b/t* and (b) *h/t*

A linear regression analysis relates the *b/t* and *h/t* ratios to the percent degradation of the maximum cyclic moment at the 0.04 rad. cycle. The *b/t* ratio appears to have a larger effect on degradation compared to the *h/t* ratio, but their slopes are similar with values of 0.011 and 0.010, respectively. The linear regression analysis results suggest that a larger value of *h/t* causes less degradation than a

comparable *b/t* value. Based on this fact, the degradation of moment capacity is found to be more dependent on the *b/t* ratio. From this analysis, recommendations for the limiting *b/t* and *h/t* ratios for seismic design can be made. To ensure that a section will have adequate ductility under large cyclic rotations, beam sections should be chosen that have *b/t* and *h/t* ratios for which the moment capacity remains above 80% of the overall maximum moment when cycled to 0.04 rad. Utilizing the linear regression analysis, sections should have a minimum *b/t* ratio of 20 and a minimum *h/t* ratio of 36 to ensure stable behavior.

3. UNREINFORCED HSS-TO-HSS MOMENT CONNECTION

Previous studies have considered the behavior of monotonically loaded unstiffened HSS-to-HSS exterior and interior connections (Korol et al. 1977). These connections are limited by several failure modes including column face plastification, chord punching shear, fracture of the beam, chord sidewall yielding, and column shear. For connections with small beam width-to-column width ratios ($\beta \leq 0.85$), the moment capacity can be determined by a yield line analysis. Connections with large beam width-to-column width ratios ($\beta > 0.85$) are limited by chord side wall failure. In order to better understand the effect of β and the depth of the connection on the cyclic hysteretic behavior, a detailed finite element model is developed and displaced cyclically to large rotations.

3.1 Connection model

The unreinforced connection model is composed of a HSS 355.6x355.6x15.9 column and nine different HSS beam members. The beam members have depths of 254.0 mm, 304.8 mm, and 355.6 mm and range in width from 101.6 mm to 304.8 mm. This allows for a wide range of β to be considered from 0.29 to 0.86. Fig. 3.1a shows an example finite element model. The column in the model is 3962 mm long and pinned at each end, while the beam member is 2870 mm long. The beam is centered and fixed to the column member along all of the beam edges utilizing a tie constraint to represent a fully welded connection. Material properties are the same as those used for the HSS beam model (Fadden and McCormick 2012b). The finite element mesh is optimized utilizing S4R shell elements and does not implement initial imperfections. The loading protocol prescribes beam tip displacements following the same protocol as shown in Fig. 2.1c producing inter-story drifts up to 0.06 rad.

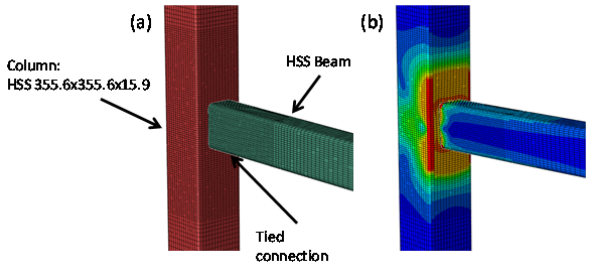

Figure 3.1 Unreinforced HSS-to-HSS exterior connection model (a) section geometry and (b) von Mises stress distribution at 0.06 rad. rotation

3.2 Unreinforced HSS-to-HSS moment connection behavior

All connections show symmetric hysteretic behavior with increasing moment capacity throughout the loading protocol. The connection with the HSS 304.8x304.8x15.9 beam member reaches the highest maximum moment of 270 kN-m at 0.06 rad. rotation, while the HSS 254.0x152.4x15.9 has the lowest maximum moment of 835 kN-m at 0.06 rad. rotation. As previously noted, the beam width-to-column width ratio (β) has an important effect on the behavior of the connection. Fig. 3.2 shows the measured moment normalized by the plastic moment capacity of the beam member versus the rotation of the connections with HSS 304.8x152.4x15.9 (β=0.43), HSS 304.8x203.2x15.9 (β=0.57), and HSS

304.8x304.8x15.9 (β=0.86) beams. As β increases from 0.43 to 0.86, the normalized maximum moment increases from 0.26 to 0.36 with larger hysteretic loops. However, the plastic moment capacity of the beam member is not fully utilized. The connection with the HSS 304.8x304.8x15.9 beam member only reaches 36% of the beam moment capacity. Further, the plastic deformation of the connection is concentrated at the column face, which is undesirable for seismic design (Fig. 3.1b).

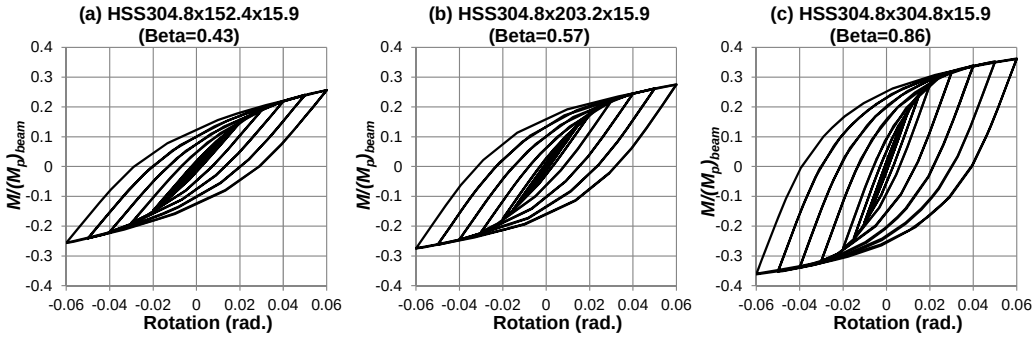

Figure 3.2 Normalized moment-rotation hysteretic behavior for the unreinforced connection with (a) HSS 304.8x152.4x15.9, (b) HSS 304.8x203.2x15.9, and (c) HSS 304.8x304.8x15.9 beams

The effect of β on the normalized maximum moment for all modelled connections is shown in Fig. 3.3a. All connections show improved maximum normalized moment with increasing β. The connection with the HSS 355.6x101.6x15.9 beam (β=0.29) reaches the lowest maximum normalized moment of 0.24, while the connection with the HSS 304.8x304.8x15.9 beam (β=0.86) reaches the highest maximum normalized moment of 0.36. The effect of increasing β on the maximum moment capacity is not linear. In connections with β smaller than 0.57, increasing the beam width does little to increase the maximum normalized moment capacity. The connection with the HSS 304.8x101.6x15.9 beam has a maximum normalized moment capacity of 0.25 and the connection with the HSS 304.8x203.2x15.9 beam has a maximum normalized moment capacity of 0.28. This is an increase of only 0.03 for an increase in β from 0.29 to 0.57. When β increases above 0.7, the increase in normalized moment capacity becomes larger. The connection with the HSS 254.0x203.2x15.9 beam has a normalized moment capacity of 0.29 at a β of 0.57 while the normalized moment capacity increases to 0.34 when a beam with a β of 0.71 is used. None of the unreinforced sections utilize the full moment capacity of the beam member even with β>0.85, showing that unreinforced connections under cyclic loads are incapable of developing the beam plastic moment capacity and the use of internal and external stiffeners is necessary

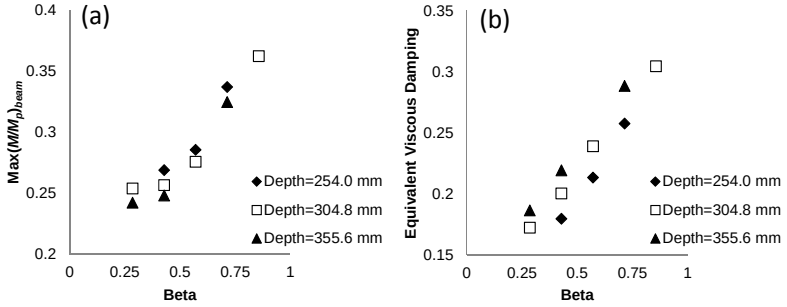

Figure 3.3. Effect of the beam width-to-column width ratio (β) on the connection (a) maximum normalized moment and (b) equivalent viscous damping

Equivalent viscous damping provides a measure of the energy dissipation capacity normalized by the elastic strain energy times 4π. Consideration of the equivalent viscous damping is important to understand the ability of the connection to dissipate energy with increasing deformation cycles. Fig. 3.3b plots the equivalent viscous damping at the first 0.06 rad. rotation cycle versus β. Increasing β causes a linearly proportional increase in the equivalent viscous damping. The connection with the

HSS 304.8x101.6x15.9 beam shows the lowest equivalent viscous damping at the 0.06 rad. cycle of 0.17, while the connection with the HSS 304.8x304.8x15.9 beam shows the highest equivalent viscous damping at the 0.06 rad. cycle of 0.30. Additionally for the same β, increasing the depth of the section leads to improved equivalent viscous damping. The HSS 254.0x152.4x15.9 beam connection has an equivalent viscous damping value of 0.18, while the HSS 355.6x152.4x15.9 beam connection has an equivalent viscous damping value of 0.22. This occurs because a deeper beam increases the yielding area of the column face. Increasing β is shown to be more effective than increasing the beam depth for equivalent viscous damping under cyclic loads for unreinforced HSS-to-HSS moment connections.

4. REINFORCED HSS-TO-HSS MOMENT CONNECTION

To improve the performance of HSS-to-HSS moment connections under cyclic loads, two rigid moment connection details were created based on previously developed HSS columns-to-wide flange beam connections (Kurobane et al. 2004). The connections (Fig. 4.1) utilize internal and external diaphragms to attempt to move forces generated by beam displacements away from the column face and into the more rigid column sidewalls. This study considers diaphragms of different lengths (l_d) and thicknesses (t_d) to better understand the effects of these parameters on the cyclic hysteric behavior. The internal diaphragm connection (Fig. 4.1a) utilizes plates that are continuous through the column. This connection requires cutting the column in two locations and reconnecting the column utilizing complete joint penetration (CJP) welds to the diaphragm plates. The external flange plate connection (Fig. 4.1b) utilizes plates that are cut to fit around the column face and sidewalls and is fillet welded into place. Both connections will utilize flare bevel groove welds between the beam and plates and fillet welds between the beam and column.

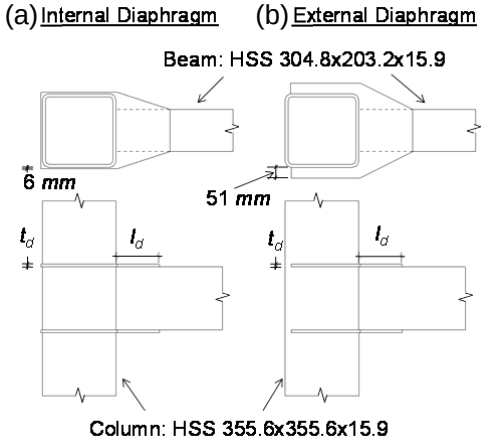

Figure 4.1 Detail for the (a) internal diaphragm and (b) external diaphragm reinforced HSS-to-HSS exterior moment connections

4.1 Connection model

The model used for the reinforced HSS-to-HSS moment connection is similar to that utilized for the unreinforced connection. Fig. 4.2a and Fig. 4.2b show the connection model for the internal and external diaphragm connections, respectively. All connections have a HSS 355.6x355.6x15.9 column with a HSS 304.8x203.2x15.9 beam providing a β of 0.57. The model utilizes shell elements for the beams and columns and C3D8H hexahedral elements for the plates. The diaphragm dimensions are shown in Fig. 4.1 where thicknesses of 9.5, 12.7, 15.9, and 19.1 mm are considered and the lengths of the diaphragm considered are 152.4, 203.2, or 254.0 mm. The material properties for the beam and columns are the same as for the beam model and the diaphragms are assumed elastic perfectly plastic with a yield stress of 250 MPa. Tie constraints are used between all adjoining edges and surfaces in the model to connect the diaphragms and members. The mesh is optimized to improve calculation speed and accuracy, but is subsequently less dense than the unreinforced connection model.

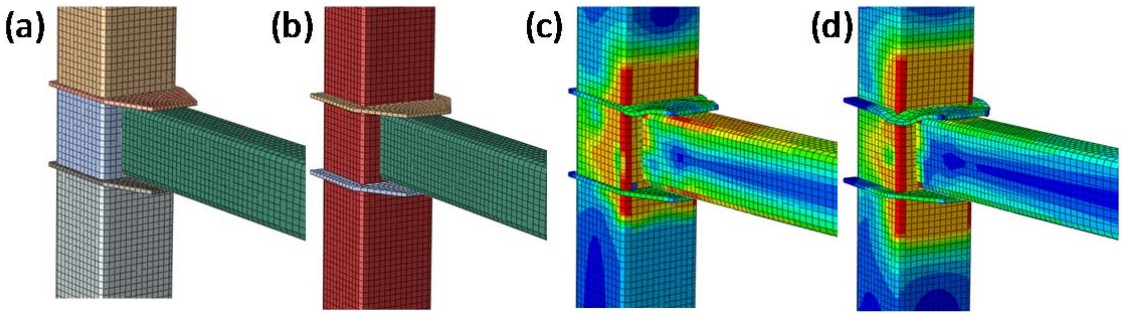

Figure 4.2 Reinforced HSS-to-HSS exterior connection model with the section geometry for the (a) internal diaphragm and (b) external diaphragm connections and von Mises stress distribution at 0.06 rad. rotation for the (c) internal diaphragm and (d) external diaphragm connections.

4.2 Internal diaphragm HSS-to-HSS moment connection behavior

All internal diaphragm connections showed symmetric cyclic hysteretic behavior with improved moment capacity over the complimentary unreinforced connection. The connection with t_d of 19.1 mm and l_d of 254.0 mm reached the highest maximum moment of 678 kN-m, while the connection with t_d of 9.5 mm and l_d of 152.4 mm achieved the lowest maximum moment of 399 kN-m. Overall, the connection performs better than the unreinforced connection by moving yielding into the beam and column sidewalls. The thickness of the internal diaphragms has an important effect on the behavior of the connection. Fig. 4.3 shows the normalized moment-rotation hysteresis for the 9.5 mm, 15.9 mm, and 19.1 mm thick diaphragms with a diaphragm length of 203.2 mm. With an increase in thickness, the normalized moment capacity increases from 0.72 for the 9.5 mm thick diaphragm to 1.21 for the 19.1 mm thick diaphragm at 0.06 rad. rotation. Additionally, as the internal diaphragm plate becomes thicker, the hysteresis loops become fuller with reduced reduction in stiffness at large rotations.

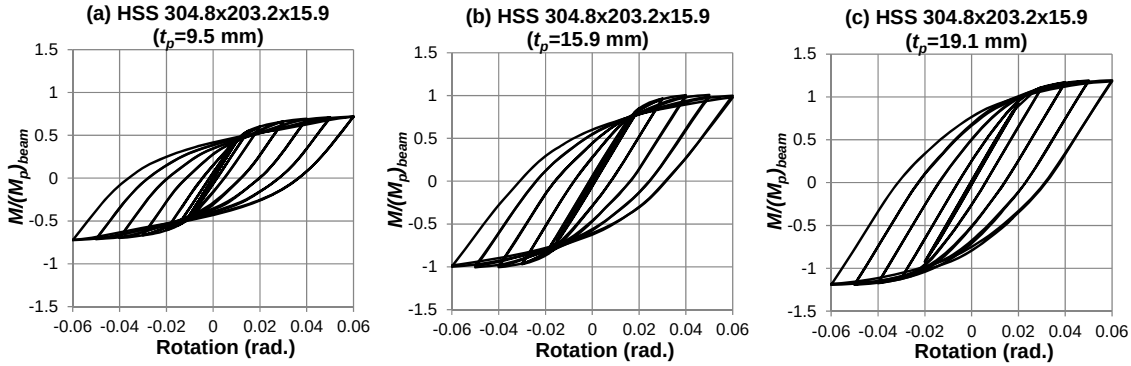

Figure 4.3 Normalized moment-rotation hysteretic behavior for the internal diaphragm connection with diaphragm thicknesses of (a) 9.5 mm, (b) 15.9 mm, and (c) 19.1 mm and a diaphragm length of 203.2 mm

The effect of the internal diaphragm thickness and length on the normalized maximum moment is shown in Fig. 4.4a. The connection with a 9.5 mm thick and 152.4 mm long diaphragm has the lowest normalized moment capacity of 0.71, while the connection with a 19.1 mm thick and 254.0 mm long diaphragm has the highest normalized moment capacity of 1.21. The length of the diaphragm is shown to have little effect on the maximum normalized moment capacity of the connection. However, an increase in the thickness of the diaphragm shows a linearly proportional increase in the normalized moment capacity. Connections with a thickness greater than or equal to 15.9 mm thick and 203.2 mm long have maximum normalized moment capacities greater than 1.0. In this case, the full plastic moment capacity of the beam member is developed, which was not achievable with the unreinforced connection.

Fig. 4.4b plots the effect of changing diaphragm thickness and length on the equivalent viscous damping capacity at a rotation of 0.06 rad. Changing thickness and length of the diaphragm has little effect on improving the equivalent viscous damping at 0.06 rad. The connection with a 15.9 mm thick, 254.0 mm long diaphragm has the minimum equivalent viscous damping of 0.24, while the connection with a 9.53 mm thick, 254.0 mm long diaphragm has the maximum equivalent viscous damping of 0.27. On average, the equivalent viscous damping is 0.26, whereas for the unreinforced connection the equivalent viscous damping is 0.23. More importantly, more yielding is occurring in the beam, column sidewalls, and diaphragms rather than at the column face where plastic deformation is undesirable.

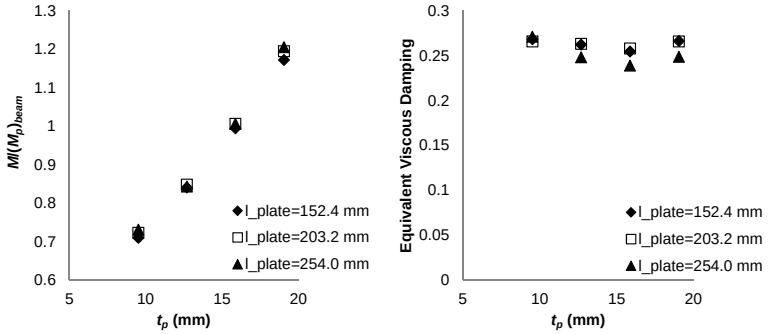

Figure 4.4 Effect of the internal diaphragm thickness and length on the (a) normalized maximum moment and (b) equivalent viscous damping of the connection

4.3 External diaphragm HSS-to-HSS moment connection behavior

External diaphragm connections show improved performance over the unreinforced connection, but not the internal diaphragm connection. The connection with t_d of 19.1 mm and l_d of 254.0 mm reached the highest maximum moment of 375 kN-m, while the connection with t_d of 9.5 mm and l_d of 152.4 mm achieved the lowest maximum moment of 251 kN-m. The connection moves some yielding into the beam and column sidewalls. As with the internal diaphragm connections, the thickness of the external diaphragms has a significant effect on the moment capacity of the connection. Fig. 4.5 shows the normalized moment-rotation hysteresis for the connections with a 9.5 mm, 15.9 mm, and 19.1 mm thick diaphragms and a diaphragm length of 203.2 mm. An increase in diaphragm thickness from 9.5 mm to 19.1 mm leads to an increase in the normalized moment capacity from 0.47 to 0.65 at 0.06 rad. rotation. Overall, all connections show full, symmetric hysteretic loops indicating stable behavior.

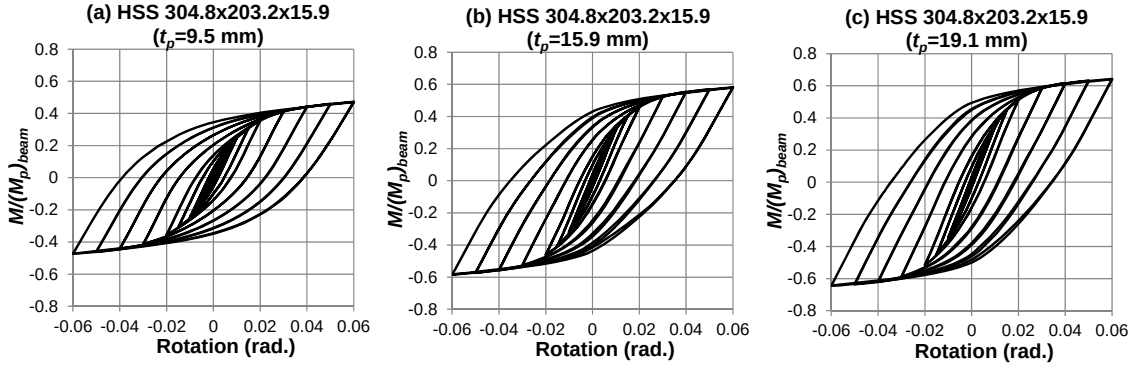

Figure 4.5 Normalized moment-rotation hysteretic behavior for the external diaphragm connection with thicknesses of (a) 9.5 mm, (b) 15.9 mm, and (c) 19.1 mm and a diaphragm length of 203.2 mm

The effect of the external diaphragm thickness and length on the normalized maximum moment is shown in Fig. 4.6a. The connection with a 9.5 mm thick and 152.4 mm long diaphragm has the lowest normalized moment capacity of 0.45, while the connection with a 19.1 mm thick and 254.0 mm long diaphragm has the highest normalized moment capacity of 0.67. Unlike the internal diaphragm connections, utilizing the external diaphragm shows improved moment capacity with increasing

diaphragm length. Increasing the diaphragm length from 152.4 mm to 254.0 mm increases the normalized moment capacity on average by 0.05 for all external diaphragm connections. Additionally, an increase in the thickness of the diaphragm shows a linearly proportional increase in the normalized moment capacity. The external diaphragm connection is unable to produce a moment capacity greater than the beam plastic moment capacity. The connection still shows considerable plastification of the column face (Fig. 4.2d). Fig. 4.6b shows that changes in length and thickness of the diaphragm plate do not cause large changes in the equivalent viscous damping capacity of the connection at 0.6 rad. rotation. On average, the equivalent viscous damping is 0.31, which is larger than the internal diaphragm connection and comparable to the unreinforced connection. In general, external diaphragm connections improve the behavior compared to the unreinforced connection, but may not be adequate to provide strong column-weak beam seismic moment frame behavior.

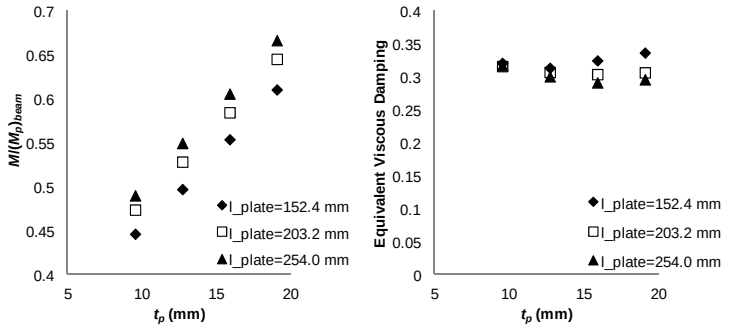

Figure 4.6 Effect of the external diaphragm thickness and length on the (a) normalized maximum moment and (b) equivalent viscous damping of the connection

5. CONCLUSIONS

The results of a finite element study considering the cyclic behavior of unreinforced and reinforced HSS-to-HSS moment connections is presented. The study utilizes findings from a previously developed HSS beam model. This model allows for the determination of limiting *b/t* and *h/t* ratios for the HSS beam member to ensure stable plastic hinging in the beam under cyclic loads. The behavior of unreinforced HSS-to-HSS moment connections is studied under cyclic loads to develop a relationship between the beam width-to-column width ratio and the load carrying capacity and equivalent viscous damping behavior. Reinforced HSS-to-HSS moment connections are then studied utilizing internal and external diaphragms to improve upon the load carrying capacity of the connection under cyclic loads. The effect of varying the diaphragm plate length and thickness on the cyclic moment capacity and equivalent viscous damping of the connection also is considered.

Overall, unreinforced and external diaphragm HSS-to-HSS moment connections are not adequate in developing the full moment capacity of the beam member. HSS-to-HSS connections utilizing internal diaphragms with diaphragm thickness and length greater than or equal to 15.9 mm and 152.4 mm, respectively, are capable of developing the full moment capacity of the beam. Internal diaphragm connection capacity is governed by diaphragm thickness, while external diaphragm connection capacity is governed by both diaphragm length and thickness. Comparing the state of stress in the member at 0.06 rad. rotation, it is clear that reinforcement helps move yielding away from the column face and into the beam and column sidewalls allowing for more desirable yielding mechanisms. Additionally, both internal and external diaphragms help improve the equivalent viscous damping capacity of the connection, but diaphragm length and thickness have little effect on this parameter. These findings further suggest the suitability of HSS-to-HSS moment connections in low-rise HSS-to-HSS seismic moment frame systems

AKCNOWLEDGEMENT
This work is supported by the BRIGE Program of the National Science Foundation under Grant No. EEC-0926858 and the American Institute of Steel Construction through the Milek Fellowship. The views expressed

herein are solely those of the authors and do not represent the views of the supporting agencies.

REFERENCES

AISC. (2006). Seismic Sesign Manual. American Institute of Steel Construction, Chicago, IL.

AISC. (2011). Manual of Steel Construction 14th Ed., American Institute of Steel Construction, Chicago, IL.

Brescia, M., Landolfo, R., Mammana, O., Iannone, F., Piluso, V., and Rizzano, G. (2009). Preliminary results of an experimental program on the cyclic response and rotation capacity of steel members. *STESSA 2009*. 971-976.

Davies, G., Packer, J.A., & Coutie, M.G. (1984). The behaviour of full width RHS cross joints. *ISTS 1984*. 411-418.

DSS (2008). Abaqus FEA Version 6.8-1 Documentation Collection. Dassault Systemes Simulia Corp. Providence, RI.

El-Tawil, S., Mikesell, T., Vidarsson, E., and Kunnath, S.K. (1998). Strength and Ductility of FR Welded-Bolted Connections Report No. SAC/BD-98/01. SAC Joint Venture, Sacramento, CA.

Fadden, M and McCormick, J. (2012a). Cyclic quasi-static testing of hollow structural section beam members. *ASCE Journal of Structural Engineering.* **138:5**, (in press).

Fadden, M and McCormick, J. (2012b) Effect of width-thickness and depth-thickness on the buckling behavior of hollow structural sections. *SSRC 2012*.

Hajjar, J.F. (2000). Concrete-filled steel tube columns under earthquake loads. *Progress in Structural Engineering and Material*. **2**, 72-81.

Hasan, S.W., and Hancock, G.J. (1988). Plastic bending tests of cold-formed rectangular hollow sections - Research report, no R586. School of Civil and Mining Engineering, University of Sydney, Sydney, Australia.

Kamba, T., Kanatani, H., and Wakida, T. (1994). CHS column-to-beam connections without diaphragms. *ISTS 1994,* 249-256.

Kamba, T., and Tabuchi, M. (1994). Database for tubular column to beam connections in moment-resisting frames. International Institute of Welding Document, no.IIW-XV-E-94-208.

Korol, R.M., and Hudoba, J. (1972). Plastic behavior of hollow structural sections. *ASCE Proceedings, Journal of the Structural Division*. **98:ST5**, 1007-1023.

Korol, R. M., El-Zanaty, M., and Brady, F.J. (1977). Unequal width connections of square hollow sections in Vierendeel trusses. *Canadian Journal of Civil Engineering,* **4:2**, 190-201.

Korol, R. M., and Mizra, F.A. (1982). Finite element analysis of RHS T-joints. *ASCE Proceedings, Journal of the Structural Division.* **108:ST9**, 2081-2098.

Koskimaki, M., and Niemi, E. (1990). Finite element studies on the behavior of rectangular hollow section K-joints. *ISTS 1990.* 28-37.

Kosteski, N., Packer, J.A., and Puthli, R.S. (2002). A finite element method based yield load determination procedure for hollow structural section connections. *Journal of Constructional Steel Research*. **59:4**, 453-471.

Kumar, S.R.S., and Rao, D.V.P. (2006). RHS beam-to-column connection with web opening-experimental study and finite element modeling. *Journal of Constructional Steel Research.* **62:8**, 739-46.

Kurobane, Y. (2002). Connections in tubular structures. *Progress in Structural Engineering*. **4**, 35-45.

Kurobane, Y., Packer, J.A., Wardenier, J., and, Yeomans, N. (2004) *Design Guide for Structural Hollow Section Column Connections.* CIDECT.

Nishiyama, I. and Morino, S. (2004). US-Japan cooperative earthquake research program on CFT structures: achievements on the Japanese side. *Progress in Structural Engineering and Materials*. **6**, 39-55.

Packer, J.A. and Henderson, J.E. (1997). *Hollow structural section connections and trusses*. Ontario, Canada: Canadian Institute of Steel Construction.

Packer, J.A. (2000). Tubular Construction. *Progress in Structural Engineering and Materials*. **2**, 41-49.

Packer, J.A., Wardenier, J., Zhao, X.L., van der Vegte, G.J., and Kurobane, Y. (2009). *Design Guide for Rectangular Hollow Sections (RHS) Joints Under Preominantly Static Loading.* CIDECT.

Rao, D.V.P., and Kumar, S.R.S. (2006). RHS beam-to-column connection with web opening-parametric study and design guidelines. *Journal of Constructional Steel Research.* **62:8**, 747-756.

Roeder, C.W. (2000). FEMA-355D State of the Art Report on Connection Performance. Federal Emaergency Management Agency, Washington, DC.

Tanaka, T., Tabuchi, M., Furumi, K., Morita, T., Usami, K., Murayama, M., and Matsubara, Y. (1996). Experimental study on end plate to SHS column connections reinforced by increasing wall thickness with one side bolted. *ISTS 1996.* 253-260.

Wilkinson, T. and Hancock, G.J. (1998). Tests to examine compact web slenderness of cold-formed RHS. *ASCE Journal of Structural Engineering*. **124:10**, 1166-1174.